A new measurement of the Cosmic-Ray Electron and Positron Spectrum with the Large Area Telescope

Alberto Manfreda
albertom@pi.infn.it

Pisa, September 21, 2016

Previous Fermi measurement of the spectrum from 7 GeV to 1 TeV published in 2010 [*Ackermann et al., Phys. Rev. D 82, 092004*]

This is a genuine new work

- Completely revised event reconstruction provided by the *Fermi* collaboration (Pass 8)
- Almost seven times the amount of data available
- Upper energy range extended to 2 TeV
- Improved selection algorithms
- Better modeling of the systematic uncertainties
- New detailed study of the geomagnetic field effects in the GeV energy range

- A tiny fraction of the cosmic-rays crowd ...

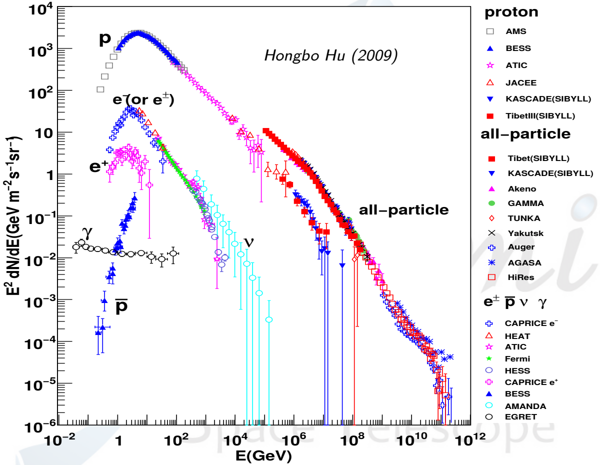

- ... but still a relevant one!

What can we study

- Injection sources (SNRs, PWN, secondary production)
  - Because of energy loss mechanisms (Inverse Compton, synchrotron emission) TeV electrons must be accelerated close (< 1 kpc) to us
  - Dominant nearby sources?
  - Exotic sources?
- Propagation models
  - Diffusion coefficient in the magnetic field
- Interaction with the heliosphere
  - Solar modulation
  - Correlation with solar cycle

What can we measure

- $e^+ + e^-$ spectrum (this work)
  - Previous Fermi and AMS02 measurements: PL with no spectral features up to 1 TeV, index ~ 3.1
  - H.E.S.S.: cutoff at 2 TeV
- Positron fraction
  - Rise of the positron fraction above ~ 10 GeV observed by Pamela, AMS02 ad Fermi
- Anisotropies
  - Expected if i.e. a single source is dominant (Vela)

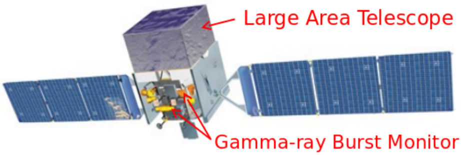

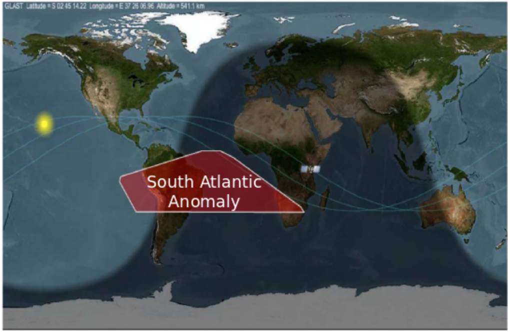

- Launch in June 2008
- Altitude : ~ 565 km
- Inclination : ~ 25.6 deg
- Period : ~ 1.5 h
- Survey mode : rocking between the northern and the southern hemispheres every orbit
- Full sky is observed every ~ 3 h
- 2 instruments: LAT and GBM, covering different energy ranges

The Large Area Telescope

- Designed mainly as a γ-ray detector
- Thanks to its calorimetric capability, can act as a detector also for electrons and positrons

Tracker/Converter

- 18 planes of silicon strip detectors
- W foils to enhance conversion probability: 1.5 radiation lengths on-axis
- 10k sensors, 80 m^2 of silicon active area, 1M readout channels

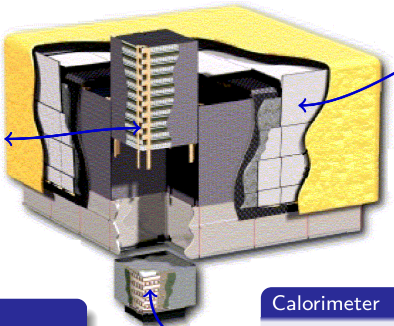

Anti-Coincidence Detector

- Segmented (89 tiles) as to minimize self-veto at high energy.
- 0.9997 average MIP detection efficiency.

A few numbers

- $\sim 1.5 \times 1.5$ m^2 area
- $\sim$ 3000 kg mass
- $\sim$ 650 W power absorbed

Calorimeter

- 1536 CsI(Tl) crystal; 8.6 radiation lengths on-axis.
- Hodoscopic, 3D shower profile reconstruction for leakage correction.

Datasets

Two different analysis, for two different datasets:

- High Energy (HE): 42 GeV - 2 TeV, using events from the standard on-board filter
- Low Energy (LE): 7 GeV - 70 GeV, using events from the diagnostic (DGN) filter

The overlap region is useful for cross-checking

- On-board filter:
  - Designed to reject charged particles (including electrons)
  - Accept all events with more than 20 GeV released in the CAL.
  - Fully efficient for electrons above $\sim$ 40 GeV
- DGN filter:
  - Unbiased sample of all triggers, pre-scaled by a factor 250

LE selection also takes into account the effect of magnetic field of the Earth

CR electrons selection:

- Trigger and event-quality cuts
- Removal of particles with Z > 1 (easy to tag by ionization in ACD and TKR)
- Main selection, using Boosted Decision Trees (BDTs), for residual hadronic contamination rejection (protons).

Event quality:

- At least on successfully reconstructed track
- Path length greater than 8 X_0 in the CAL, removing evts close to the edges or not well reconstructed
- Minimum quality of direction reconstruction

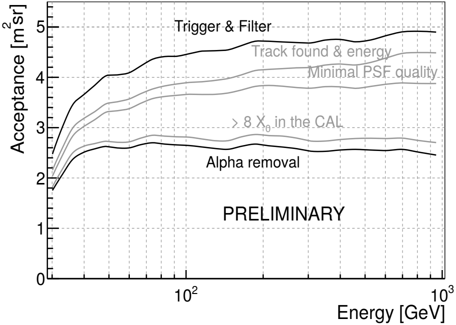

- Exploits differences between leptonic and hadronic events in the detector:
  - Shower development in the CAL
  - Number of δ-rays produced in the TKR
- Plus a few variables describing the event position in the LAT

PDG values of X_0 and λ for the CsI

X_0	1.85 cm	$8.39\ \mathrm{g \cdot cm^{-2}}$
λ	38.04 cm	$171.5\ \mathrm{g \cdot cm^{-2}}$

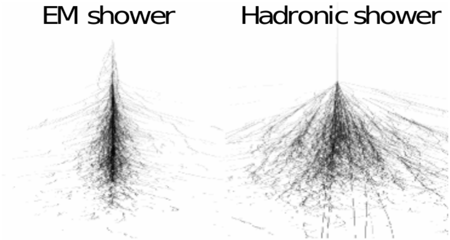

- 19 input variables used for the HE analysis, 7 for LE
- The BDT combines all the information in one variable (P_{BDT})
- 8 BDTs used for HE analysis, in different log(E) bins, to capture the change in event topology

BDT output

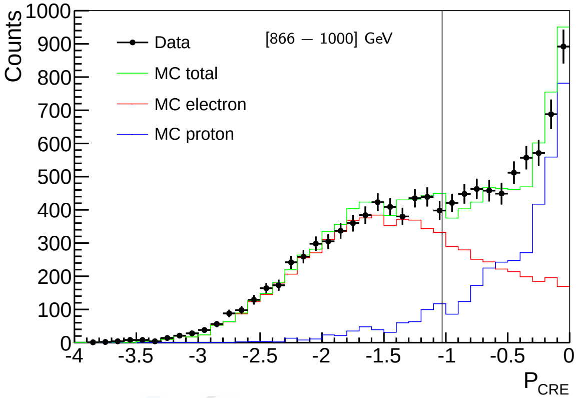

- We use $\log_{10}(1 - P_{BDT})$ to optimize the selection
- Normalization of Monte Carlo templates fitted to data in each energy bin.
- Normalization factor used in bkg estimation (subtracted form data)

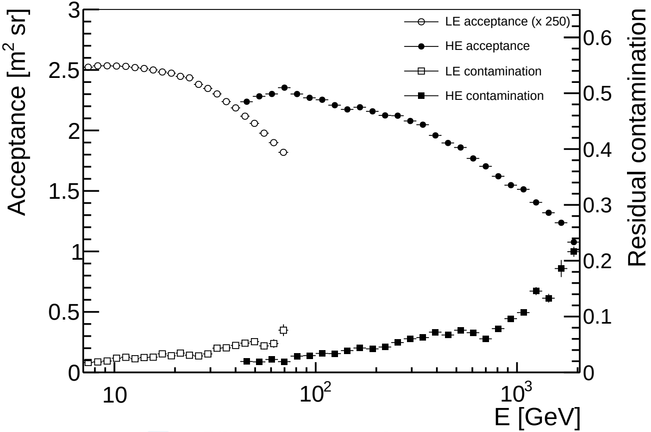

- Selection progressively more difficult at higher energy
- Contamination below 20% in the whole energy range

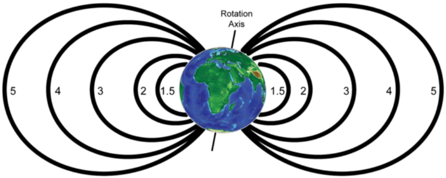

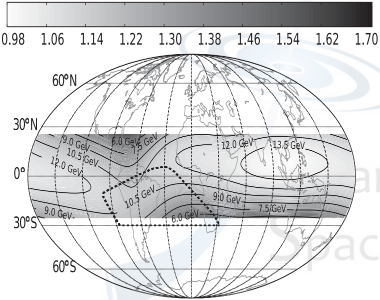

McIlwain L and rigidity cut-off values across the LAT orbit

- GeV range: shielding effect of the Earth magnetic field
- Rigidity cut-off varying with coordinates, need to select 'good' regions
- McIlwain L parameter: field lines intersection with the equatorial plane in units of earth radii
- Position with same L-value are equivalent to incoming charged particles
- LAT orbit: 0.98 - 1.73 L, vertical rigidity cut-off from $\sim$ 6 GeV to $\sim$ 14 GeV.

LE Orbital Selection (2)

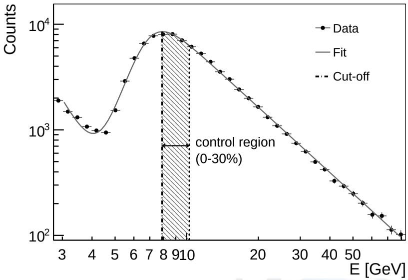

- Fit count spectrum in several McIlwain L bins
- Determine a relation between McIlwain L and energy cut-off E_c
- In each energy bin find the L_{min} value corresponding to the lower boundary of the bin
- Select $L > L_{min}$ in each energy bin

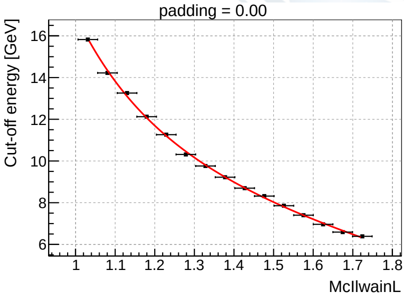

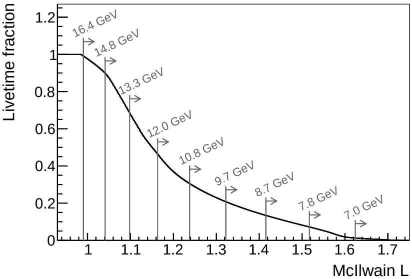

- Above the cut-off, there is still a fraction of particles lost, which can be estimated with a tracing technique
- Simulated realistic flux of $e^+ + e^-$ in the LAT, traced back in a model of the Earth magnetic field

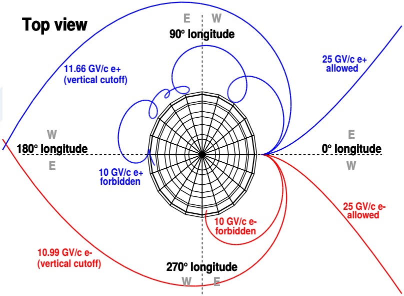

- Particles escaping to infinity correspond to allowed trajectories
- Particles reaching the Earth, or trapped, correspond to trajectories blocked by the magnetic field
- The fraction of forbidden trajectories gives an estimate of the missing flux fraction
- Spectrum is corrected to compensate for this loss

Geomagnetic correction (2)

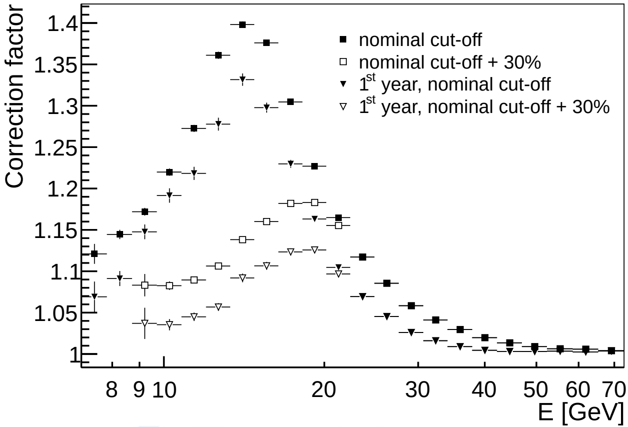

- Correction factors up to 40%, correction definitely needed!
- Separate correction factors for the first year (rocking angle changed from 35 to 50 degrees)

Systematics uncertainties

- Acceptance uncertainty:
  - Estimated by changing the selection cut and studying the resulting flux variation
  - $< 2\%$ up to ~ 500 GeV, increasing to 6% at 2 TeV
- Residual bkg uncertainty:
  - Geant4 uncertainties in modeling the most 'electron-like' fraction of proton showers
  - Estimated signal events variation $< 2\%$ up to 1 TeV (subdominant), increases to 7% at 2 TeV
- Energy scale bias uncertainty:
  - The absolute energy scale of the LAT is measured in-flight at 10 GeV by comparing the cut-off energy observed with predictions from simulation
  - The uncertainty is estimated to be 2% at 10 GeV
  - At 1 TeV, studying the distribution of quantities related to the shower profile shape, the uncertainty is estimated to be 6%

Systematics uncertainties (2)

- Variable calibration uncertainty (HE analysis):
  - The calibrations are shifts of the variables as function of energy and angle, derived to improve data/MC agreement
  - Uncertainty is estimated by bracketing the nominal set of corrections with two alternative ones, designed to encompass any residual data/MC discrepancy
  - Signal variation with this increases from 2% at 42 GeV to 10% at 1 TeV, reaching 14% at 2 TeV

- Geomagnetic corrections uncertainty (LE analysis):
  - Estimated by shifting the estimated cut-off position of [0-30%] and redoing the analysis
  - Large variation of geomagnetic correction factors
  - Flux variation is less than 3% across the whole energy range

- Counts $\mu_i(\boldsymbol{\theta})$ predicted by a given input model are fitted to the observed counts N_i
- Predicted counts computation takes into account geometrical cross section of the LAT, interaction probability, selection efficiency, instrument live time and energy dispersion effect
- No absolute energy scale uncertainty in fits: handled by changing the energy of all events (according to different scenarios) and redoing the analysis
- Errors δN_i are the quadratic sum of the statistical and acceptance uncertainties (of all the uncertainties for LE)
- Contamination and IVC correction uncertainties are included as nuisance parameters (HE only)

$$\chi^2 = \sum_{i=1}^{n} \left(\frac{N_i - [1 + s(E_i; \mathbf{w}) S(E_i)]\mu_i(\boldsymbol{\theta})}{\delta N_i} \right)^2 + \sum_{j=1}^{\mathcal{N}} w_j^2$$

Nuisance parameters

- $\mathcal{S}(E)$ is the quadratic sum of the estimated contamination and IVC correction uncertainties as a function of energy
- We model the contribution of these uncertainties with a piecewise function, $s(E;\mathbf{w})$, linear in $\log_{10}(E)$ between a certain number $\mathcal{N}$ of fixed energies
- $s(E;\mathbf{w})$ is uniquely defined by its value at the reference energies, so $\mathcal{N}$ is the number of nuisance parameters
- The correction to the predicted number of counts is $[1+s(E_i;\mathbf{w})S(E_i)]$
- The set of w_j are the nuisance parameters

$$\chi^2 = \sum_{i=1}^{n}\left(\frac{N_i - [1+s(E_i;\mathbf{w})S(E_i)]\mu_i(\boldsymbol{\theta})}{\delta N_i}\right)^2 + \sum_{j=1}^{\mathcal{N}} w_j^2$$

Nuisance parameters

- Number of nuisance parameters $\mathcal{N}$ rather arbitrary
- 8 BDTs trained in the HE range
- However, correlation between adjacent bins is expected: lower numbers seem more reasonable
- We used $\mathcal{N} = 6$ and tested the stability of all results with $\mathcal{N} = 5,7$

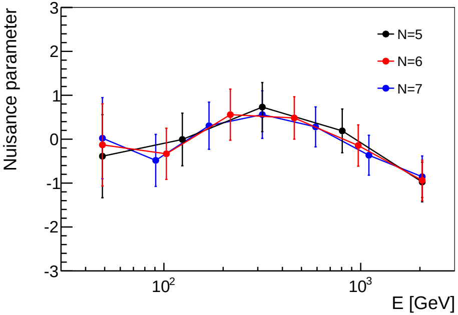

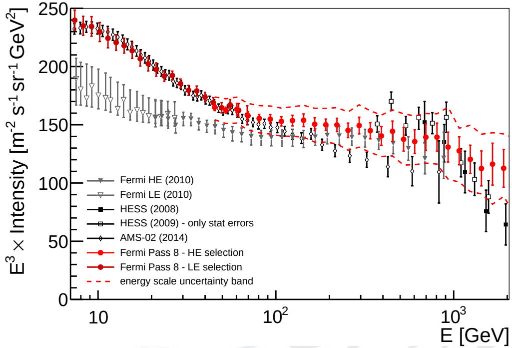

- Input model: PL of index −3.1 fitted *individually in each energy bin* (only for displaying the data points)
- Error bars: stat+syst uncertainties summed in quadrature
- Dashed lines: energy scale varying linearly in $log_{10}(E)$ between −2% at 10 GeV and −6% at 1 TeV and between +2% at 10 GeV and +6% at 1 TeV

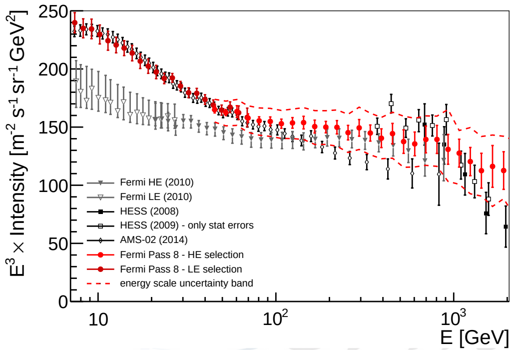

- Good agreement of the two analysis in the overlapping region
- Disagreement between old and new Fermi points below $\sim$ 100 GeV
  - Geomagnetic correction
  - Imperfections in the simulation that was used in the previous analysis (remnants of electronic signals from out-of-time particles were not simulated)

Results

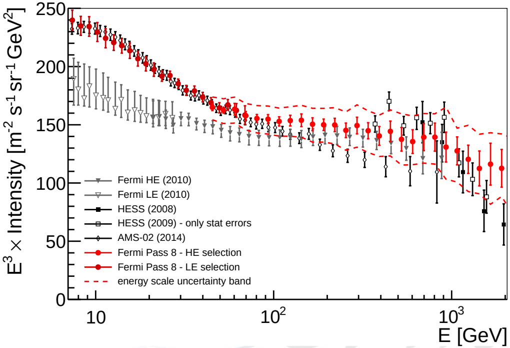

- Single PL fit in the whole range: $\chi^2 = 64.6$ for 36 d.o.f
- Broken PL fit: $\chi^2 = 19.2$ for 34 d.o.f
- Break at 53 ± 8 GeV, indices are 3.21 ± 0.02 below and 3.07 ± 0.02 above
- However, not significant when including energy scale uncertainty

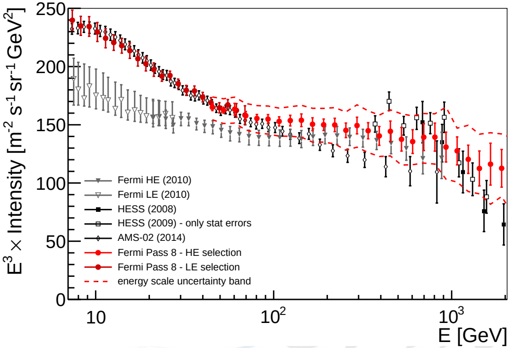

- Between 50 GeV and 2 TeV, the CRE spectrum is compatible with a single power law with a spectral index of 3.07 ± 0.02 (stat+syst)
- Including energy scale uncertainty the index may vary between 3.01 and 3.13

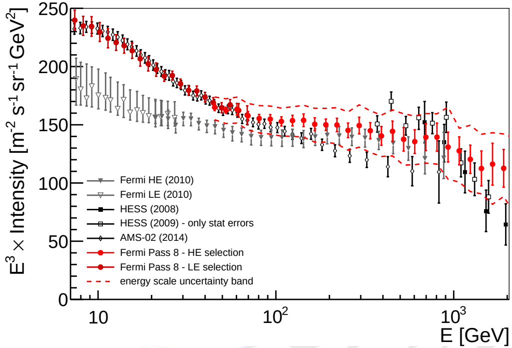

- Fitting with $E^{-\gamma}e^{-E/E_c}$ to test exponential cut-off hypothesis:
  - $E_c < 2.1$ TeV is excluded at 95% CL
  - Assuming a scenario in which the energy scale is changed by $+2\%$ at 50 GeV to -6% at 1 TeV, $E_c < 1.7$ TeV is excluded at 95% CL

Conclusions

- I have presented a measurement of the CRE spectrum between 7 GeV and 2 TeV with the LAT
- Analysis have been finalized
- Will be object of a paper (submitted for peer-review in the next few days)
- A search of anisotropies using the CRE selection developed for this analysis is currently under preparation by the Fermi collaboration (not personally involved)
- Future developments: looking for effects of solar modulation below 20 GeV
  - No significant deviation from PL behavior observed in current work (uncertainties are too high)
  - Looking for time variations of the flux, likely connected with solar cycle